

CHEMICAL EVOLUTION OF ODD ELEMENTS IN AN INHOMOGENEOUS EARLY GALAXY

Takuji TSUJIMOTO

*National Astronomical Observatory, Mitaka-shi, Tokyo 181-8588, Japan
taku.tsujimoto@nao.ac.jp*

Toshikazu SHIGEYAMA

*Research Center for the Early Universe, Graduate School of Science, University of Tokyo, Bunkyo-ku, Tokyo 113-0033, Japan
shigeyama@astron.s.u-tokyo.ac.jp*

and

Yuzuru Yoshii

*Institute of Astronomy, Graduate School of Science, University of Tokyo, Mitaka-shi, Tokyo 181-8588, Japan
yoshii@ioa.s.u-tokyo.ac.jp*

(Received 22 June 2001; accepted 12 September 2001)

Abstract

We investigate the chemical evolution of odd-numbered elements such as sodium (Na) and aluminum (Al) during the early epochs of the Galactic halo with the use of a model that reproduces the observed box-shaped distribution of extremely metal-poor stars in the [Na, Al/Mg] versus [Mg/H] plane. Our model is constructed under the assumptions that those stars retain the elemental abundance patterns produced by *individual* Type II supernovae (SNe), and that the yields of the odd elements depend on the initial metallicity, z , of their SN progenitors. As a result, recent abundance determinations that clarify how the [Na, Al/Mg] ratios of field stars have evolved to the solar values enable us to deduce how the yields of these odd elements depend on z . The observed trends in these abundances, in particular the very large scatter (over 1 dex in [Al/Mg]) requires that the Al yield scales as $m_{\text{Al}} \propto z^{0.6}$ for $[\text{Mg}/\text{H}] \lesssim -1.8$, while the observed [Na/Mg] trend requires that the Na yield scales as $m_{\text{Na}} \propto z^{-0.4}$ for $[\text{Mg}/\text{H}] \lesssim -1.8$ and $m_{\text{Na}} \propto z^{0.4}$ for $[\text{Mg}/\text{H}] \gtrsim -1.8$. It is found that the predicted frequency distribution of stars in the [Na/Mg] versus [Mg/H] diagram is very sensitive to the assumed form of the primordial IMF, and that its slope is *steeper than the Salpeter IMF*. The necessity to match the observed abundance patterns of odd elements and the frequency distribution of extremely metal-poor stars should provide useful constraints on nucleosynthesis calculations of metal-free massive stars as well as on theories of their formation.

Key words: Galaxy: evolution — Galaxy: halo — stars: abundances — stars: Population II — supernovae: general — supernova remnants

1. INTRODUCTION

Recent high-resolution observations of metal-poor halo stars show that the relative abundances of certain elements of odd nuclear charge number, specifically sodium (Na) and aluminum (Al), as compared with that of even nuclear charge number elements like magnesium (Mg), are on the average smaller than the solar ratio, with large star-to-star variations. In particular, the scatter covers a range of $-1 < [\text{Na}/\text{Mg}] < 0$ and $-1.5 < [\text{Al}/\text{Mg}] < 0$, far exceeding errors in abundance measurements for stars with $[\text{Mg}/\text{H}] \lesssim -2$ (McWilliam et al. 1995) (see also Norris, Ryan, & Beers 2001). This observed feature of Na and Al in very metal-poor stars (which may partially originate from abundance measurements based on very few lines, including resonance lines) has yet to be fully explained with present chemical evolution models of the Galactic halo.

The elements Na, Mg, and Al, in order of increasing charge number, are produced as a result of hydrostatic carbon and neon burning in massive stars – supernova

(SN) explosions merely expel these elements without affecting their yields (Pagel 1997 and references therein). While Mg is a primary element, both Na and Al are secondary elements in the sense that their production depends on the amount of seed heavy elements contained in the initial chemical composition of the SN progenitor star. Theoretical calculations of SN models indeed indicate the existence of an odd-even effect, such that the predicted abundance ratios of [Na/Mg] and [Al/Mg] are smaller for lower metallicity stars, where metallicity is indicated by [Mg/H] (Arnett 1971; Woosley & Weaver 1982). However, in order to make the odd-even effect compatible with the large observed variation in [Na/Mg] and [Al/Mg] for $[\text{Mg}/\text{H}] \lesssim -2$, chemical inhomogeneity in the Galactic halo gas at early epochs needs to be introduced, otherwise [Na/Mg] and [Al/Mg] would show a very tight correlation with [Mg/H], which is not seen.

One mechanism for introducing the required inhomogeneity is the model of chemical evolution proposed by Tsujimoto, Shigeyama, & Yoshii (1999, hereafter TSY99;

2000, hereafter TSY00), in which each SN event triggers star formation in the swept-up gas, so that newly formed stars inherit the elemental abundance pattern of individual SNe (Shigeyama & Tsujimoto 1998; Tsujimoto & Shigeyama 1998; Nakasato & Shigeyama 2000). Argast et al. (2000) also constructed a 3D stochastic chemical evolution model that can incorporate the inhomogeneity introduced by individual SN explosions. This kind of inhomogeneous models has successfully reproduced the observed variety of abundance patterns of α -elements and iron-peak elements, based on theoretical SN yields of these heavy elements, which are presently calculated with reasonable accuracy. It is important to note that, because abundance patterns for extremely metal-poor stars should retain the fossil record of the nucleosynthesis of their individual SN progenitors, the inhomogeneous model is a useful tool for deducing the production sites and yields of other elements for which SN models have not yet provided consistent results (TSY00).

Significant progress has been made in nucleosynthesis calculations based on SN progenitors with various metallicities and masses, but theoretical SN yields of odd elements such as Na and Al have not yet converged to consistency among models from different authors (Woosley & Weaver 1995; Limongi et al. 1998; Umeda, Nomoto, & Nakamura 2000). Limongi et al. (1998) and Umeda et al. (2000) predict that both the synthesized masses of Al and Na for $20 M_{\odot}$ SN model increase by a factor of ~ 3 – 4 as the metallicity increases from zero to $z=0.05z_{\odot}$. On the other hand, Woosley & Weaver (1995) show that for a $22 M_{\odot}$ SN model, the amount of Al is insensitive to the metallicity for the range of $z = 0 - 0.01z_{\odot}$, whereas the amount of Na *decreases* by a factor of ~ 25 with increasing metallicity in the same range. In addition, there has also been significant progress in observational abundance determination of these elements, providing new information on elemental abundance trends for both extremely metal-poor stars as well as higher metallicity disk stars (Pilachowski, Sneden, & Kraft 1996; Hanson et al. 1998; Fulbright 2000). These observations show how the [Na, Al/Mg] ratios of field halo stars have evolved to the solar values. The results are intriguing. A tight correlation of [Al/Mg] ratios with [Mg/H] starts at [Mg/H] ~ -1.8 , with the values of [Al/Mg] higher than those of most extremely metal-poor stars populating the boxed-shape distribution, whereas for [Na/Mg] the trend starts to change at [Mg/H] ~ -1.8 towards the solar metallicity while gradually reducing their star-to-star variation of [Na/Mg]. This might imply a different z -dependence between the Al and Na yields in the metal-poor regime.

The purpose of this paper is to *empirically* determine the Al and Na yields that can account for the observed abundance trends in the context of the inhomogeneous chemical evolution model proposed by TSY99 and TSY00. In this model, new stars are formed following each SN event, thus their abundance pattern is determined by the combination of heavy elements ejected from the SN itself and those elements which are already present in the interstellar gas swept up by the supernova remnant (SNR).

The predicted stellar abundance patterns are thus different from those of the gas at the time when stars form. This difference can be quite large in the early stage of Galactic evolution, when the metallicity in the gas is very low. The abundance ratios of low-metallicity stars are predicted to exhibit a large star-to-star scatter, depending in detail on the abundance patterns of SN ejecta with different progenitor masses. In the later phase, the predicted scatter in abundance ratios becomes smaller toward larger [Mg/H], which is ascribed to the switch of the major contribution to stellar metallicity from the ejecta of SNe to the metallicity in the interstellar gas swept up by SNRs.

In §2 we derive the metallicity-dependent Na and Al yields. In §3 we construct a model for the evolution of Na and Al that is fully consistent with the large star-to-star variation in [Na/Mg] and [Al/Mg] observed for metal-poor stars. Our conclusions are presented in §4.

2. EMPIRICAL DETERMINATION OF SN YIELDS OF ODD ELEMENTS

According to our understanding of the early evolution of the Galaxy, there must presently exist long-lived second-generation stars with surface abundance patterns that exactly reflect the yields of odd elements from individual SNe of Population III (Pop III SNe). Such stars populate the branch associated with the production of element X and Mg from individual Pop III SNe in the [X/Mg] versus [Mg/H] diagram. We refer to this branch as the y -branch (the letter y stands for its origination in individual SNe II yields), from which the yield of element X from Pop III SNe can adequately be derived (TSY00).

The seed element for Al production is Mg, while that for Na production is Ne, whose abundance is unfortunately difficult to measure for metal-poor stars. We therefore note that the odd-even effect, which would remain only indicative in the [Na/Mg] ratio, is best investigated with the [Al/Mg] ratio. Hence, in this section we first discuss Al and then Na.

2.1. Aluminum

Figure 1a shows the values of [Al/Mg] plotted against [Mg/H] for a sample of stars (Edvardsson et al. 1993; McWilliam et al. 1995; Fulbright 2000)¹ that covers the full metallicity range. Contrary to the small scatter in [Al/Mg] for [Mg/H] $\gtrsim -1.8$, the values of [Al/Mg] for [Mg/H] $\lesssim -1.8$ scatter over 1 dex at any given [Mg/H].

There are two remarkable features clearly separated at [Mg/H] ~ -1.8 in the [Al/Mg] versus [Mg/H] diagram: (1) A lack of correlation between [Al/Mg] and [Mg/H] for stars with [Mg/H] $\lesssim -1.8$, indicated by the shaded area, and (2) a tight correlation for stars with [Mg/H] $\gtrsim -1.8$, as expected from the odd-even effect. The first feature occurs as a result of chemical inhomogeneity in the halo (TSY99, TSY00). The second feature occurs due to the

¹ Here we limit the data to a body of tens of stars in order to avoid the scatter originating from differences in the values reported by different authors.

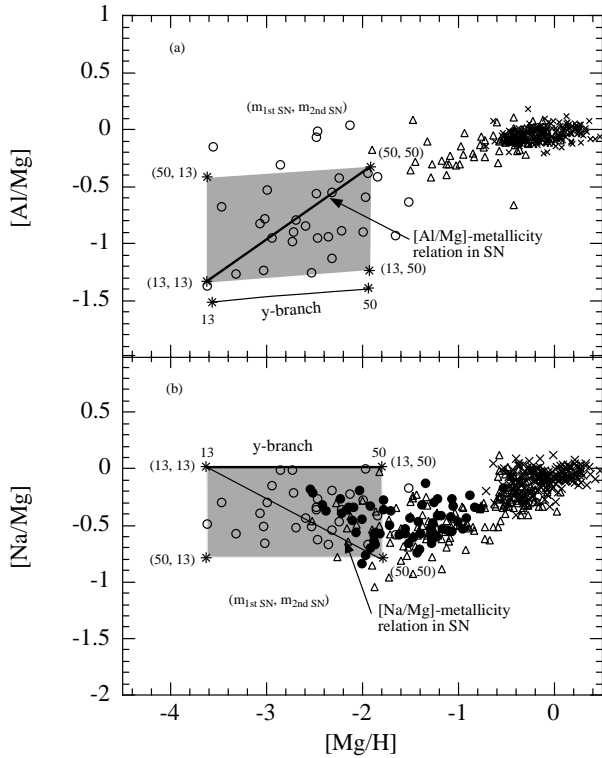


Fig. 1. (a) The observed correlation of $[\text{Al}/\text{Mg}]$ with $[\text{Mg}/\text{H}]$ (open circles; McWilliam et al. 1995, open triangles; Fulbright 2000, crosses; Edvardsson et al. 1993). The thin line indicates the y -branch for Pop III SNe, while the thick line represents the relation between synthesized $[\text{Al}/\text{Mg}]$ and *initial* metallicity $[\text{Mg}/\text{H}]$ in SN progenitors. The shaded area cornered with asterisk symbols is the predicted location of the stars born in the first few generations (b) The same as (a) but for Na. Other observed data (filled circles; Hanson et al. 1998) are added.

fact that the stellar metallicity is determined by the metallicity in the interstellar gas swept up by SNRs, instead of that in the ejecta of individual SNe. Through the transition from feature 1 to 2, mixing of SN products from all previous nucleosynthesis sites with the ISM gradually weakens the chemical inhomogeneity introduced by individual SNe. However, the gradual mixing process is not seen in the $[\text{Al}/\text{Mg}]$ - $[\text{Mg}/\text{H}]$ distribution in the metallicity range $-3.6 \lesssim [\text{Mg}/\text{H}] \lesssim -1.8$ because the first few generation stars overlap in this metallicity region (the shaded region of Fig. 1a) as described below. Therefore the second feature appears for stars with $[\text{Mg}/\text{H}] \gtrsim -1.8$.

Theoretical SN models show that values of $[\text{Al}/\text{Mg}]$ originating from Pop III SNe with different progenitor masses are similar, exhibiting differences of at most ~ 0.4 dex. Thus we assume that stars born in SNRs of Pop III progenitor stars have an almost constant $[\text{Al}/\text{Mg}]$. Since there is no way to populate stars below the y -branch owing to

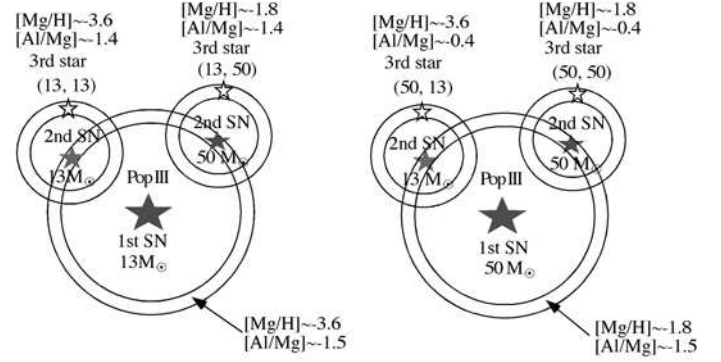


Fig. 2. Schematic illustration of the SN-induced star formation model, indicating elemental abundance patterns for second- and third-generation stars. The left shows the case for third-generation stars born in the SNRs from progenitor stars having masses of 13 and 50 M_{\odot} , which are born in the SNR of a Pop III progenitor star having a mass of 13 M_{\odot} . The right shows the same as the left but for a Pop III progenitor star having a mass of 50 M_{\odot} . Concentric circles, filled stars, and open stars denote SNR shells, SNe, and newly-formed stars, respectively.

the odd-even effect, we need to locate the y -branch, as indicated by the thin line, just below the data points in Figure 1a. The thick line in this figure indicates the relation between synthesized $[\text{Al}/\text{Mg}]$ and *initial* metallicity $[\text{Mg}/\text{H}]$, which SNe should satisfy in order to reproduce the observed scatter in $[\text{Al}/\text{Mg}]$. Given this metallicity-dependent Al yield, we can account for the resultant distribution of long-lived stars in the $[\text{Al}/\text{Mg}]$ versus $[\text{Mg}/\text{H}]$ diagram.

Second-generation stars located along the y -branch have $[\text{Al}/\text{Mg}] \sim -1.4$ by assumption, but have various metallicities, indicated by $[\text{Mg}/\text{H}]$, over a range of almost 2 dex (the thin line in Fig. 1a). For example, because SNe with larger progenitor masses eject a larger amount of metals, second-generation stars born in the SNR of a Pop III progenitor star having a mass of 50 M_{\odot} have $[\text{Mg}/\text{H}] \sim -1.8$ on the right end of the y -branch, and those stars from a 13 M_{\odot} SN have $[\text{Mg}/\text{H}] \sim -3.6$ on the left end.

As schematically illustrated in Figure 2, third-generation stars born in the SNR from a progenitor star with a higher metallicity, of order $[\text{Mg}/\text{H}] \sim -1.8$, must have a higher ratio of $[\text{Al}/\text{Mg}] \sim -0.4$ due to the metallicity-dependent Al yield. On the other hand, stars of the same generation from a progenitor star with lower metallicity, $[\text{Mg}/\text{H}] \sim -3.6$, must have a lower ratio of $[\text{Al}/\text{Mg}] \sim -1.4$, which is similar to that of second-generation stars on the y -branch. In either instance, apart from $[\text{Al}/\text{Mg}]$, stars that originated from SN explosions must have very different metallicities of $[\text{Mg}/\text{H}]$ if the progenitor stars have different masses.

In this way, the location of a star in the $[\text{Al}/\text{Mg}]$ versus $[\text{Mg}/\text{H}]$ diagram is determined by the combination of progenitor masses of SNe of the preceding two gen-

erations. In particular, third-generation stars are distributed in the shaded area in Figure 1a, with its corners labelled by asterisk symbols and the parenthetic quantities ($m_{1\text{st SN}}, m_{2\text{nd SN}}$). For example, stars near (50, 13) originate from SNe with progenitor masses of $13 M_{\odot}$, which are in turn the offspring of Pop III SNe with progenitor masses of $50 M_{\odot}$. Since stars of later generations show similar abundance distributions, gradually shifting towards higher $[\text{Mg}/\text{H}]$, the first three generations suffice to basically reproduce the observed star-to-star variation in $[\text{Al}/\text{Mg}]$.

Consequently, the lack of a tight correlation between $[\text{Al}/\text{Mg}]$ and $[\text{Mg}/\text{H}]$ for $[\text{Mg}/\text{H}] \lesssim -1.8$ can be understood as arising from two independent factors: (1) The metallicity, $[\text{Mg}/\text{H}]$, of a star, determined by the progenitor masses of the SN from which the star was formed, and (2) the abundance ratio $[\text{Al}/\text{Mg}]$ of the same star, determined by the *initial* metallicity of each SN progenitor.

Finally, we should note the problem of determining the Al abundance based on resonance lines. For the metal-poor stars observed by McWilliam et al. (1995), the Al abundances are necessarily determined from resonance lines, since other lines used in Fulbright (2000) and Edvardsson et al. (1993), which give much more reliable abundances, lie below the detection limit. Baumüller & Gehren (1997) have demonstrated that the LTE analysis for these resonance lines leads to considerable underestimation $\Delta[\text{Al}/\text{H}] \sim -0.65$ for stars with $[\text{Fe}/\text{H}] \lesssim -2$. Details of how such a non-LTE effect changes the distribution of $[\text{Al}/\text{Mg}]$ has been investigated by Norris et al. (2001) and shown in their Figure 8. Their result implies that there is no change in the overall trend of $[\text{Al}/\text{Mg}]$ represented by the above two features, but with a somewhat smaller scatter in $[\text{Al}/\text{Mg}]$ for extremely metal-poor stars, i.e., $\Delta[\text{Al}/\text{Mg}] \sim 0.7$ rather than $\Delta[\text{Al}/\text{Mg}] \sim 1.0$.

2.2. Sodium

Figure 1b shows the values of $[\text{Na}/\text{Mg}]$ plotted against $[\text{Mg}/\text{H}]$ for metal-poor halo stars (McWilliam et al. 1995) and disk stars (Edvardsson et al. 1993). Thanks to the available $[\text{Na}/\text{Mg}]$ data for $-2.5 \lesssim [\text{Mg}/\text{H}] \lesssim -1$ (Hanson et al. 1998, which is a revised version of data from Pilachowski et al. 1996) for halo and disk stars, as well as the data of Fulbright (2000), we clearly see the observational trend of $[\text{Na}/\text{Mg}]$ over the whole metallicity range. We stress that the abundance determinations of Na by the above authors, which determine the overall trend of $[\text{Na}/\text{Mg}]$, are based on lines that are little affected by conditions of non-LTE. A smaller scatter in $[\text{Na}/\text{Mg}]$ compared with $[\text{Al}/\text{Mg}]$ for $[\text{Mg}/\text{H}] \lesssim -1.8$ indicates that the Na yield is less sensitive to metallicity than the Al yield in the metal-poor regime.

The box-shaped distribution for $[\text{Mg}/\text{H}] \lesssim -1.8$ can in principle be reproduced by either the horizontal y -branch on the bottom side of the box, and the upward diagonal reflecting larger Na yields for higher metallicity (similar to the Al case in Fig. 1a), or the horizontal y -branch on the top side of the box and the downward diagonal reflecting a smaller Na yield for higher metallicity stars. However, the

requirement of a continuous transition at $[\text{Mg}/\text{H}] \sim -1.8$ (e.g., from feature 1 to feature 2 – see §2.1–) results in our preference of the latter alternative. The adopted y -branch is shown by the thin line in Figure 1b, and the required metallicity-dependence of the Na yield is indicated by the thick line, which seems to be at variance with expectations from the odd-even effect.

We note that current SN models give discrepant results for the Na yield; Umeda et al. (2000) claimed an increasing trend of Na yield as a function of metallicity, but Woosley & Weaver (1995) claimed an decreasing trend in the metal-poor regime followed by an increasing trend towards higher metallicity (see Fig.18 of Timmes, Woosley, & Weaver 1995). Although this theoretical discrepancy needs to be resolved by more detailed nucleosynthesis calculations, the observed $[\text{Na}/\text{Mg}]$ distribution for metal-poor stars might provide compelling evidence in favor of the decreasing trend of Na yields.

3. INHOMOGENEOUS CHEMICAL EVOLUTION OF ODD ELEMENTS IN THE GALACTIC HALO

In this section we discuss the inhomogeneous chemical evolution of odd elements in the Galactic halo, based on the formulation presented in TSY99. The essence of the picture is that the star-forming process is confined in separate clouds which make up the entire halo, and that the chemical evolution in these clouds proceeds through repetition of successive sequence of SN explosion, shell formation, and star formation therein. All Pop II stars are assumed to form in SNR shells. Heavy elements ejected from an SN are assumed to be trapped and well-mixed within the SNR shell. Some of these elements go into stars of the next generation, and the rest is left in the gas that will be mixed with the ambient medium. Thus the abundance of heavy element i in stars, $z_{i,*}(m, t)$, born at time t from an SNR shell with progenitor mass m , is defined as

$$z_{i,*}(m, t) = \frac{M_{z_i}(m) + z_{i,g}(t)M_{\text{sw}}(m, t)}{M_{\text{ej}}(m) + M_{\text{sw}}(m, t)}, \quad (1)$$

where $M_{z_i}(m)$: the mass of synthesized heavy element i ejected from a star with mass m , $z_{i,g}(t)$: the abundance of heavy element i in the gas, $M_{\text{sw}}(m, t)$: the mass of the shell formed at time t from an SN with progenitor mass m , and $M_{\text{ej}}(m)$: the mass of the SN ejecta. Details can be found in TSY99.

The free parameters in the inhomogeneous model are the mass fraction x_{III} of metal-free Pop III stars initially formed in each cloud, and the mass fraction ϵ of stars formed in the dense shells swept up by each SNR. We take $x_{\text{III}} = 2.5 \times 10^{-4}$, which is consistent with the observed level of $[\text{Ba}/\text{Mg}]$ for the i -branch (TSY00). We take $\epsilon = 4.3 \times 10^{-3}$ in order to reproduce the observed metallicity distribution function of metal-poor halo stars (TSY99). The initial stellar mass function (IMF) used here is a Salpeter one with upper and lower mass limits of $50M_{\odot}$ and $0.05M_{\odot}$, respectively. The lower mass limit

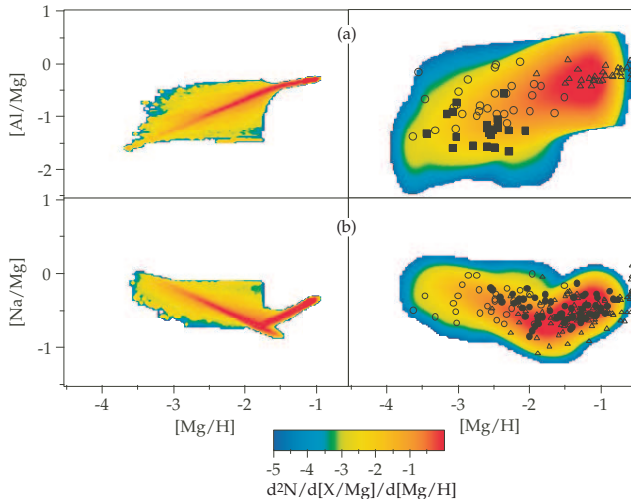


Fig. 3. (a) Color-coded frequency distribution of the long-lived stars in the $[\text{Al}/\text{Mg}]$ - $[\text{Mg}/\text{H}]$ plane, convolved with a Gaussian having $\sigma = 0.3$ dex for $[\text{Al}/\text{Mg}]$ and $\sigma = 0.1$ dex for $[\text{Mg}/\text{H}]$ (right panel), and without convolution (left panel). The symbols represent the same data which as in Figure 1. Other observed data (filled squares; Ryan, Norris, & Beers 1996) are added. (b) The same as (a) but for Na. The $[\text{Na}/\text{Mg}]$ ratios are convolved with $\sigma = 0.1$ dex in the right panel.

of stars that explode as SNe is taken to be $10M_{\odot}$.

First, relating the synthesized Mg mass m_{Mg} to the mass m of the SN progenitor star, and also to the Mg abundance of a SNR shell from which stars are born (Shigeyama & Tsujimoto 1998), the y -branch in the $[\text{Al}/\text{Mg}]$ versus $[\text{Mg}/\text{H}]$ diagram can be converted into the Al yield of Pop III SNe, denoted by $m_{\text{Al,III}}$ as a function of m . Next, using the diagonal shown by the thick line in Figure 1a, the metallicity-dependent Al yield is taken as $m_{\text{Al}}(m, [\text{Mg}/\text{H}]) = m_{\text{Al,III}}(m) \times 10^{0.6([\text{Mg}/\text{H}] + 3.7)}$, or $m_{\text{Al}} \propto z^{0.6}$, scaling with some power of the initial metallicity z of the SN progenitor star. If the observed scatter of $[\text{Al}/\text{Mg}]$ for metal-poor stars is reduced as expected by the non-LTE effect on the Al abundances (Norris et al. 2001), the metallicity-dependence on the Al yield becomes small. For instance, the $[\text{Al}/\text{Mg}]$ distribution obtained by Norris et al. (2001), which is taken into account non-LTE effect by Baumüller & Gehren (1997), yields $m_{\text{Al}} \propto z^{0.4}$.

Adopting the Al yield m_{Al} as a function of m and z obtained as above, we calculate the expected frequency distribution of stars in the $[\text{Al}/\text{Mg}]$ versus $[\text{Mg}/\text{H}]$ diagram. The left panel of Figure 3a shows the color-coded distribution after normalization to unity when integrated over the entire area. In order to enable a direct comparison with the data, the distribution has to be convolved with Gaussian errors having $\sigma = 0.3$ dex for $[\text{Al}/\text{Mg}]$ and $\sigma = 0.1$ dex for $[\text{Mg}/\text{H}]$. The right panel of Figure 3a shows this convolved distribution, which agrees well with the distribution of the observed data.

Similar to the case of Al, by using the y -branch and the diagonal metallicity trend for Na in Figure 1b, we obtain the metallicity-dependent Na yield as $m_{\text{Na}} \propto z^{-0.4}$ for

$[\text{Mg}/\text{H}] \lesssim -1.8$, which reverses to become $m_{\text{Na}} \propto z^{0.4}$ for $[\text{Mg}/\text{H}] \gtrsim -1.8$. We then calculate the expected frequency distribution of stars to be compared with the data in the $[\text{Na}/\text{Mg}]$ versus $[\text{Mg}/\text{H}]$ diagram, and find that a steeper IMF for metal-free Pop III stars enhances the variation in $[\text{Na}/\text{Mg}]$. As discussed in §2.1, the stellar distribution in the $[\text{Na}/\text{Mg}]$ - $[\text{Mg}/\text{H}]$ plane for $[\text{Mg}/\text{H}] \leq -1.8$ can be basically described by third-generation stars. All second-generation stars populate on the thick line $[\text{Na}/\text{Mg}] \sim 0$ in Figure 1b. The $[\text{Na}/\text{Mg}]$ ratio of each star of the third generation is determined by the yields of these elements from the preceding SN (2nd SN in Fig. 1b) and the amounts of Na and Mg in the ISM eventually swept up by this SN. It is found that the Salpeter IMF makes the contribution of Na and Mg in the ISM to the $[\text{Na}/\text{Mg}]$ ratios of third-generation stars significant, and the values of $[\text{Na}/\text{Mg}]$ approach ~ 0 (thick line in Fig. 1b). On the other hand, a steep IMF decreases the fraction of Pop III stars that undergo SN explosion, so that Na and Mg in the ISM cannot contribute to the $[\text{Na}/\text{Mg}]$ ratios of third-generation stars. As a consequence, third-generation stars could populate the full range of the shaded region in Figure 1b. Therefore, this dependence can be used to constrain the IMF slope for the massive part, i.e., $m \geq 10M_{\odot}$ from the $[\text{Na}/\text{Mg}]$ versus $[\text{Mg}/\text{H}]$ diagram. For example, the IMF slope index for Pop III stars of $x = -1.8$ results in the frequency distribution shown in Figure 3b. To be consistent with the box-shaped distribution observed for $[\text{Mg}/\text{H}] \lesssim -1.8$, we conclude that the primordial IMF should be more inclined than the Salpeter IMF.

4. SUMMARY AND DISCUSSION

Based on the hypothesis that early generations of stars are born from individual SNRs in the young Galaxy, we have explored the nature of the abundance trends seen in odd elements such as Na and Al. We have found that the combination of SN-induced star formation and metallicity-dependent yields of odd elements from SNe can account for the large variation in $[\text{Na}/\text{Mg}]$ and $[\text{Al}/\text{Mg}]$ observed for extremely metal-poor halo stars. The Al yield, required to reproduce the observed star-to-star variation spanning $-1.5 < [\text{Al}/\text{Mg}] < 0$ for $[\text{Mg}/\text{H}] \lesssim -1.8$, should scale with the initial metallicity z of SN progenitor stars as $m_{\text{Al}} \propto z^{0.6}$. The Na yield, required to reproduce the variation of $-1 < [\text{Na}/\text{Mg}] < 0$, should scale as $m_{\text{Na}} \propto z^{-0.4}$ for $[\text{Mg}/\text{H}] \lesssim -1.8$ and $m_{\text{Na}} \propto z^{0.4}$ for $[\text{Mg}/\text{H}] \gtrsim -1.8$.

An inverse z -trend of the Na yield, which decreases with increasing z for the metal-poor stars, is obtained from observations of $[\text{Na}/\text{Mg}]$ – this may be understood if the Na production on its seed Ne is exceeded by the α -capture of Ne into Mg. Our result agrees with nucleosynthesis calculations of massive stars by Woosley & Weaver (1995), but it is, on the other hand, at variance with other calculations by Umeda et al. (2000). A definitive confirmation of our result therefore requires more detailed nucleosynthesis calculations.

We found that the box-shaped distribution of extremely metal-poor stars in the $[\text{Na}/\text{Mg}]$ versus $[\text{Mg}/\text{H}]$ diagram

constrains the slope of primordial IMF to be steeper than the Salpeter IMF. This suggests that metal-free stars beyond $50M_{\odot}$ are significantly deficient, as advocated from theoretical study of star formation in metal-free gas (Yoshii & Sabano 1979; Yoshii & Saio 1986).

[Al/Mg] ratios that are above the solar value are not predicted in our model of inhomogeneous chemical evolution, unless a large observational error is allowed for. However, Iwamoto et al. (2001) showed that if efficient internal mixing processes occur, the Al abundance of a stellar surface whose metallicity is $[Mg/H] \sim -3.5$ is enhanced up to $[Al/Mg] \sim 0$ during later phases of stellar evolution. Their result implies the possible existence of stars having more enhanced Al abundances if stronger mixing takes place in their stellar interiors. In this regard, it should be noted that the red giant stars of globular cluster M13 exhibit an anomalously high [Al/Mg] ratio in the abundance range $0 \lesssim [Al/Mg] \lesssim 1.3$ (e.g., Kraft et al. 1997; Norris & Da Costa 1995), which does not overlap at all with $-1.5 \lesssim [Al/Mg] \lesssim 0$ observed for field halo stars. Moreover, such an Al overabundance relative to Mg in globular cluster stars is anti-correlated with metallicity (Gratton et al. 2000), which indicates the enhanced production of odd elements by *p*-capture processes taking place deep inside (Cavallo, Sweigart, & Bell 1996), followed by mixing due to meridional circulation and turbulent diffusion driven by stellar rotation (Denissenkov & Tout 2000, Zahn's mechanism). Some indication that globular cluster stars indeed rotate while field stars do not (Kraft et al. 1997) partly justifies preferential acquisition of angular momentum by protostellar fragments in dense environments. Thus, the origin of anomalously high [Al/Mg] ratios seen in globular cluster stars is more local and can be separated from that seen in field halo stars related to the global chemical evolution of the Galactic halo.

We are grateful to Timothy C. Beers for his careful reading and helpful comments. This work has been partly supported by COE research (07CE2002) and a Grant-in-Aid for Scientific Research (11640229) of the Ministry of Education, Science, Culture, and Sports in Japan.

References

- Argast, D., Samland, M., Gerhard, O. E., & Thielemann, F.-K. 2000, *A&A*, 356, 873
- Arnett, W. D. 1971, *ApJ*, 166, 153
- Baumüller, D., & Gehren, T. 1997, *A&A*, 325, 1088
- Baumüller, D., Butler, K., & Gehren, T. 1998, *A&A*, 338, 637
- Cavallo, R. M., Sweigart, A. V., & Bell, R. A. 1996, *ApJ*, 464, L79
- Denissenkov, P. A., & Tout, C. A. 2000, *MNRAS*, 316, 39
- Edvardsson, B., Andersen, J., Gustafsson, B., Lambert, D. L., Nissen, P. E., & Tomkin, J. 1993, *A&A*, 275, 101
- Fulbright, J. P. 2000, *AJ*, 120, 1841
- Gratton, R. G., Sneden, C., Carretta, E., & Bragaglia, A. 2000, *A&A*, 354, 169
- Hanson, R. B., Sneden, C., Kraft, R. P., & Fulbright, J. 1998, *AJ*, 116, 1286
- Iwamoto, N., et al. 2001, in preparation
- Kraft, R. P., Sneden, C., Smith, G. H., Shetrone, M. D., Langer, G. E., & Pilachowski, C. A. 1997, *AJ*, 113, 279
- Limongi, M., Straniero, O., & Chieffi, A. 1998, in *Stellar Evolution, Stellar Explosions and Galactic Chemical Evolution*, ed. A. Mezzacappa (Institute of Physics Publishing: London), 385
- McWilliam, A., Preston, G. W., Sneden, C., & Searle, L. 1995, *AJ*, 109, 2757
- Nakasato, N., & Shigeyama, T. 2000, *ApJ*, 541, L59
- Norris, J. E., & Da Costa, G. S. 1995, *ApJ*, 441, L81
- Norris, J. E., Ryan, S. G., & Beers, T. C. 2001, submitted to *ApJ*
- Pagel, B. E. J. 1997, *Nucleosynthesis and Chemical Evolution of Galaxies* (Cambridge University Press)
- Pilachowski, C. A., Sneden, C., & Kraft, R. P. 1996, *AJ*, 111, 1689
- Ryan, S. G., Norris, J. E., & Beers, T. C. 1996, *ApJ*, 471, 254
- Shigeyama, T., & Tsujimoto, T. 1998, *ApJ*, 507, L135
- Timmes, F. X., Woosley, S. E., & Weaver, T. A. 1995, *ApJS*, 98, 617
- Tsujimoto, T., & Shigeyama, T. 1998, *ApJ*, 508, L151
- Tsujimoto, T., Shigeyama, T., & Yoshii, Y. 1999, *ApJ*, 519, L64 (TSY99)
- Tsujimoto, T., Shigeyama, T., & Yoshii, Y. 2000, *ApJ*, 531, L33 (TSY00)
- Umeda, H., Nomoto, K., & Nakamura, T. 2000, in *The First Stars*, ed. A. Weiss, T. Abel & V. Hill (Heidelberg: Springer), 150
- Woosley, S. E., & Weaver, T. A. 1982, in *Essays in Nuclear Astrophysics*, ed. D. N. Schramm, 377
- Woosley, S. E., & Weaver, T. A. 1995, *ApJS*, 101, 181
- Yoshii, Y., & Sabano, Y. 1979, *PASJ*, 31, 505
- Yoshii, Y., & Saio, H. 1986, *ApJ*, 301, 587